

## Investigation of potential fields anomalies related with the Philippi basin and granitoid intrusion, NE Greece

A. Stampolidis, G. N. Tsokas, G. Eleftheriadis and D. Kondopoulou

Geophysical Laboratory, Aristotle University of Thessaloniki, 54006, Thessaloniki, Greece

Received 1 November 2000; accepted 15 April 2000

**Abstract:** Gravity and magnetic data were used in the study of Philippi basin and intrusion. The most rigorous methods were used for the recompilation of the aeromagnetic map of Macedonia and Thrace. Philippi basin has a maximum depth of about 5.4 km. The aeromagnetic data reveal the presence of a large intrusion, much greater than the two small granitic outcrops.

**Key Words:** Philippi, Granitoid, Potential Fields, N. Greece

### INTRODUCTION

Philippi basin (Fig. 1) is situated in the western part of the Rhodope Massif, which mainly consists of Meso-

zoic to Paleozoic medium to high grade metamorphic rocks and extends along Greek-Bulgarian borders, also occupying a small part of NW Turkey. This basin, and

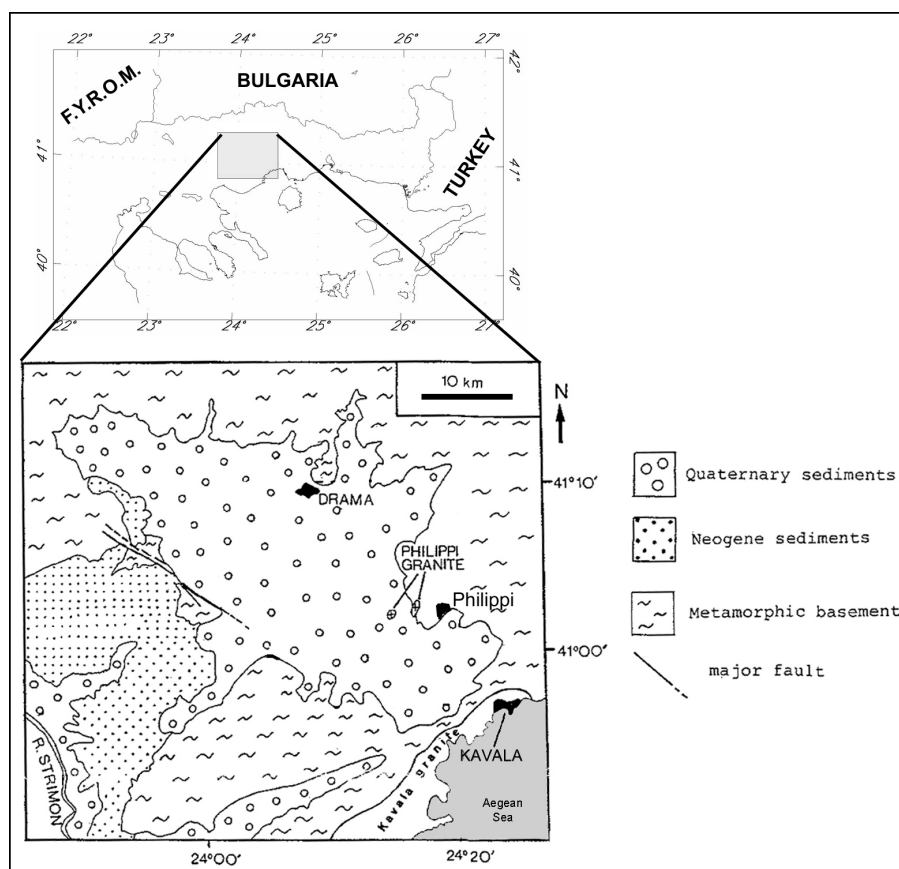


**FIG. 1.** Simplified geological map of the Philippi basin. The locations of the two small granitic outcrops near Philippi village are also visible.

the Strimon basin to the west, have a NW-SE orientation parallel to the Hellenides. It was initiated in the Late Miocene by reactivation of basement faults. The Philippi pluton is one of many Tertiary intrusions in the Rhodope massif (Bitsios *et al.*, 1981; Zachos and Dimadis, 1983).

Philippi basin is an asymmetric graben of Miocene-Quaternary age. Time of initiation of this basin coincides with a tensional phase in the Aegean area, which resulted in the formation of a series of basins (Lyberis, 1984). There is a system of NW-SE trending normal faults at the western edge of the basin, whilst the eastern part of the basin is an associated rollover structure with limited antithetic faulting. The crystalline basement of the Rhodope zone surrounds the basin. The sedimentary infill of the basin consists predominantly of fluvial and lacustrine deposits.

The Philippi granitoid intrudes marbles and schists of the Lower Tectonic Unit of the Rhodope massif (Papanikolaou and Panagopoulos, 1981), causing intensive contact metamorphism phenomena. According to Eleftheriadis *et al.* (1995), the abundance of microgranular enclaves and absence of schistosity characterize the granitoid. Extensional partial melting of source mantle that was hornblende-rich as a result of earlier subduction derived both enclaves and granitoids. The total surface outcrop of the intrusive rocks is about 1 km<sup>2</sup>. The granitoid has been dated to 26-28 Ma by K/Ar method (Kronberg *et al.*, 1970; Bitsios *et al.*, 1981).

The present work is aimed to study the sedimentary cover of the Philippi basin and the concealed granitic intrusion by means of potential field analyses and modeling.

## DATA USED

The Bouguer anomaly data used in this study were extracted from the Greek gravity data bank that Lagios *et al.* (1994) made available to the public. They recompiled the Bouguer anomaly

map of Greece using the data of a previous map (Makris and Stavrou, 1984), augmented by the data of more recent industrial surveys. The latter were mainly carried out by the

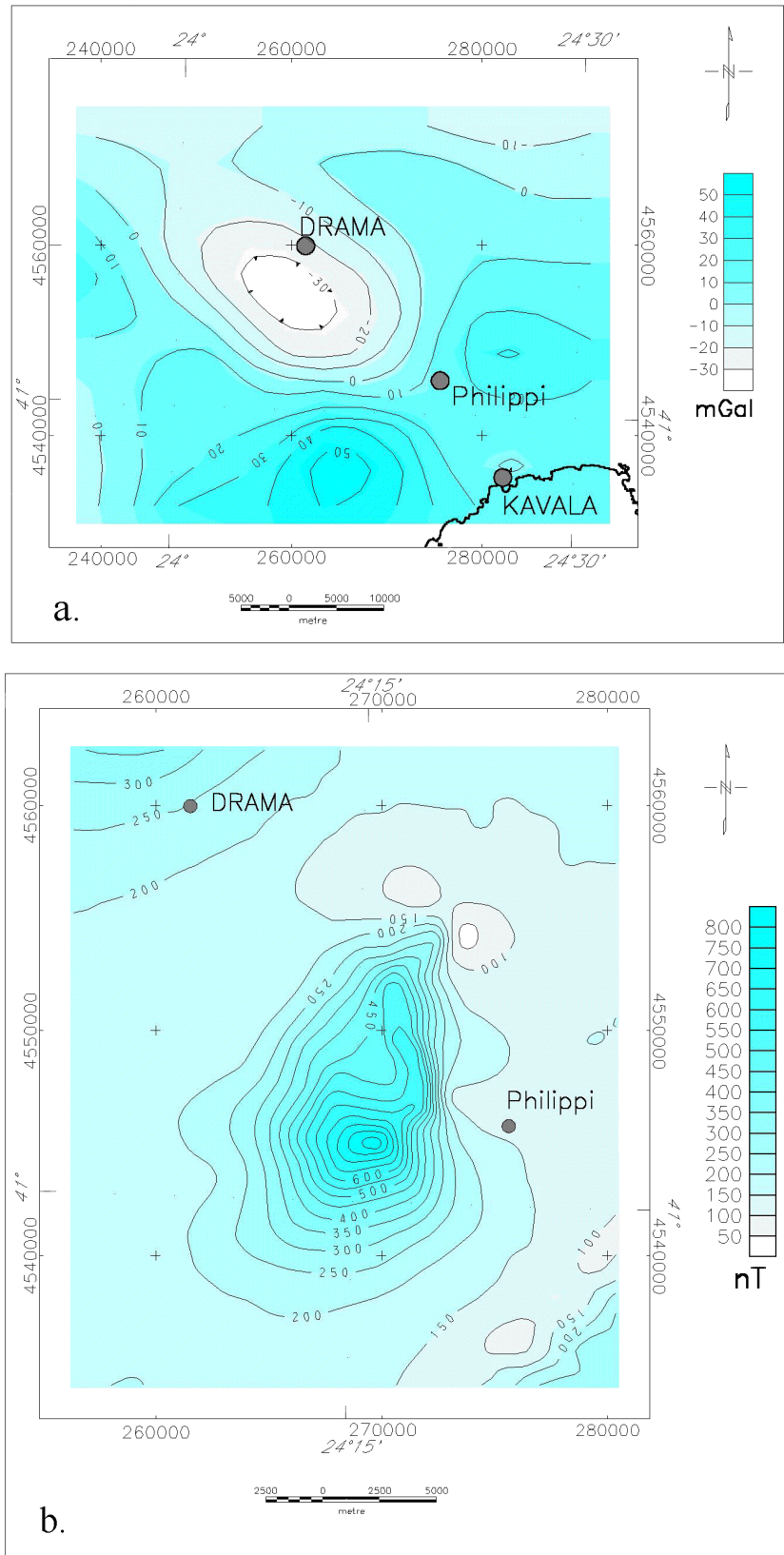


**FIG. 2.** Bouguer anomaly map of Philippi area, (a). Total field anomaly map of Philippi area (b).

Institute for Geology and Mineral Exploration of Greece (IGME) and the Public Petroleum Company (DEP-EKY). The offshore shipborne data were digitized from maps of Morelli *et al.* (1975a, b). The map compiled from this data set is shown in Figure 2a.

A uniform density contrast between sediments and metamorphic rocks was chosen after Maltezos (1987). The value of the contrast was put to  $-0.35 \text{ g/cm}^3$ . Maltezos (1987) and Maltezos and Brooks (1989) attempted forward modeling to the Philippi anomaly using this density contrast, and found a maximum depth of 6 km, they also suggested that there was no density contrast between Philippi pluton and the surrounding rocks.

The aeromagnetic data used here were produced in 1966 during a campaign of ABEM-Elektrisk Malmetning Company on behalf of IGME (ABEM 1967). Flight lines were flown in WSW-ENE direction, perpendicular to the regional strike of the Hellenides. They were spaced 0.8 km apart and tie lines were flown at a spacing of 30 km. A constant clearance altitude of  $275 \pm 75 \text{ m}$  above ground level was maintained throughout the survey.

Stampolidis (1999) digitized the original hardcopy profiles. The resulted total field magnetic profiles were subjected to a series of corrections. The DGRF model (1966.5) was subtracted from the data, lag and heading corrections applied also. Next, tie line leveling was performed and finally microleveling applied in order to remove the high frequency noise from the magnetic data. The total field magnetic anomaly map of Philippi is shown in Figure 2b.

Atzemoglou (1997) conducted apparent magnetic susceptibility and remanence magnetization measurements at the Philippi intrusion. The mean susceptibility value of the granitoid was found to be  $\kappa = 31.4 \cdot 10^{-3} \text{ (SI)}$ , close to that measured in other Oligocene granitic intrusion of Rhodope massif. The maximum measured remanence intensity was  $J_r = 550 \text{ mA/m}$  but some

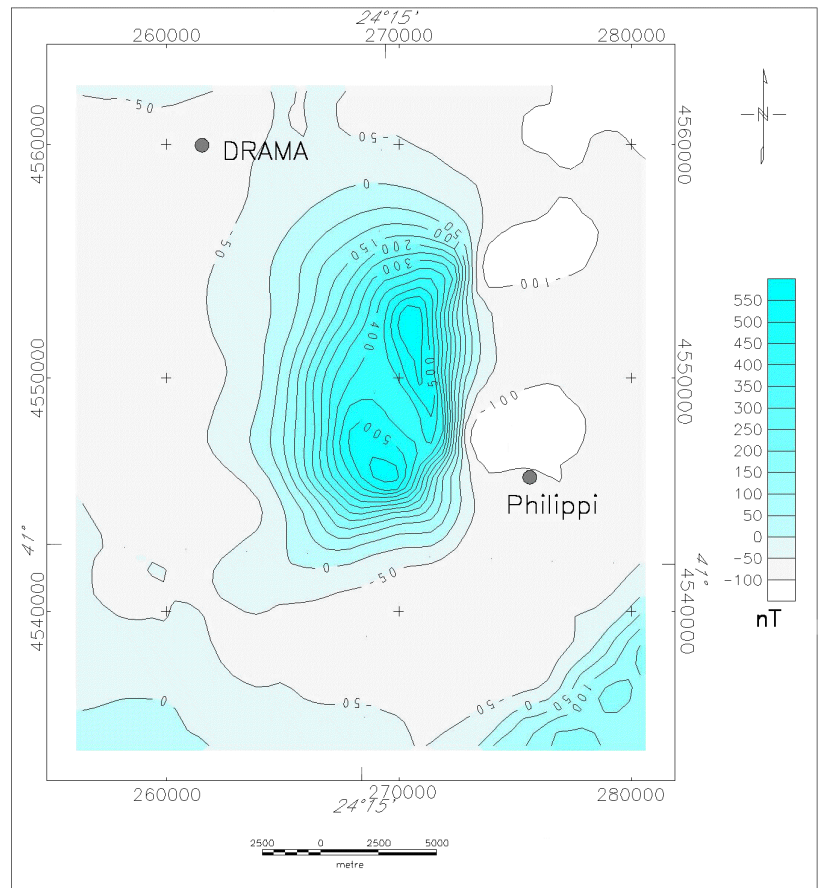


**FIG. 3.** Reduced to the north magnetic pole total field anomaly map of Philippi.

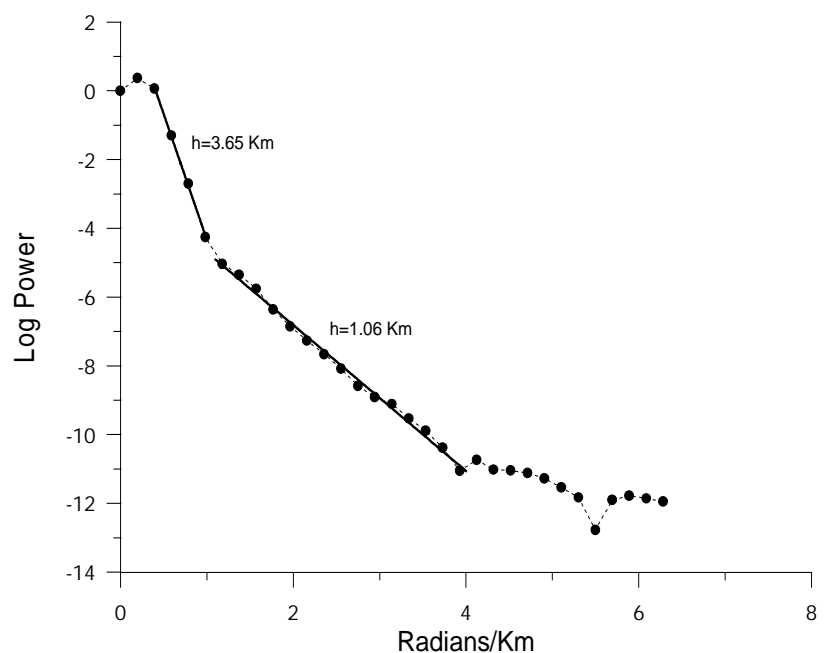


**FIG. 4.** Azimuthally averaged logarithmic power spectrum of the reduced to the pole total field data. The fitted straight-line segments are also shown.



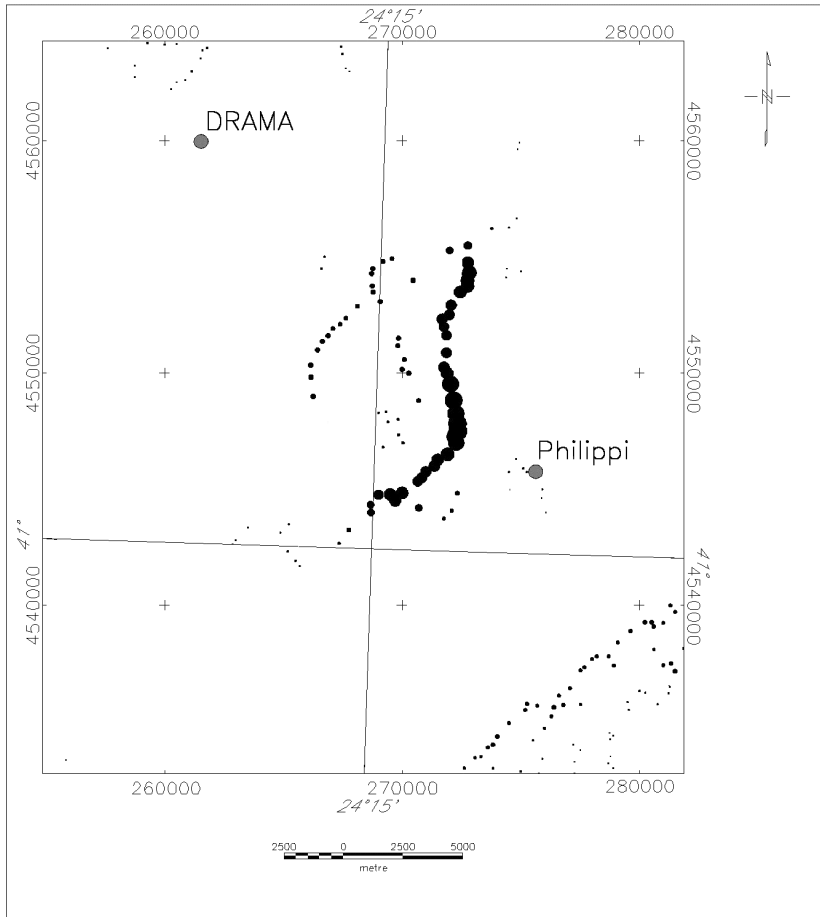


**FIG. 5.** Horizontal Gradient Maxima map.

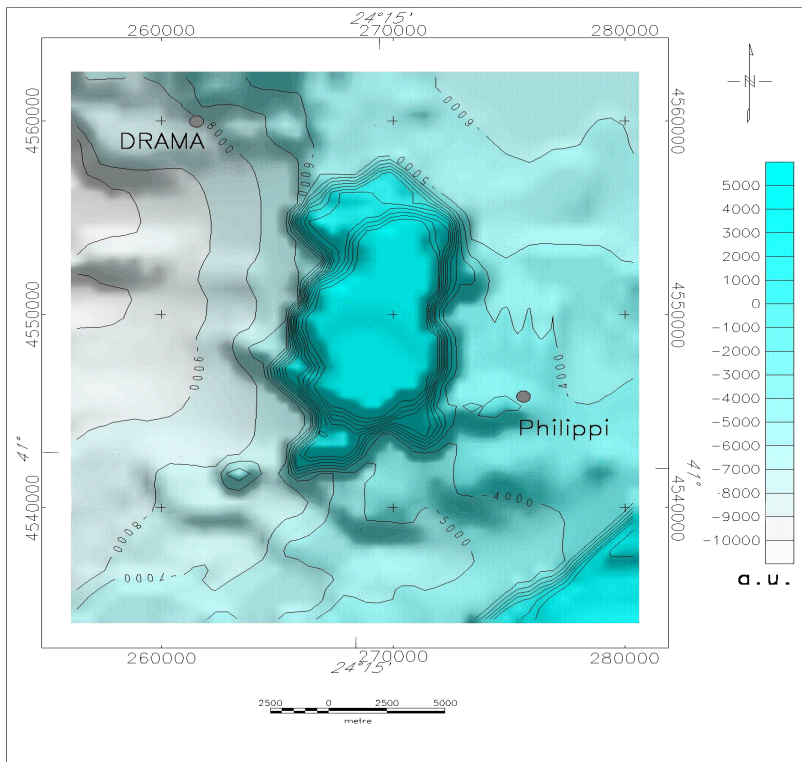


**FIG. 6.** "Terraced" magnetic field of Philippi. Units are arbitrary.

samples displayed very low values (about 3 mA/m). The mean declination of magnetization was  $D=25^\circ$  and the mean inclination  $I = 66^\circ$ . The Koenigsberger ratio was  $Q = 0.38$ . Magnetic mineralogy experiments (e.g. thermoremanent analysis, isothermal remanent acquisition) have shown that magnetite is the main carrier of magnetization.

### PROCESSING OF THE ANOMALOUS POTENTIAL FIELDS

Processing of the data was carried out using both Potential Field Geophysical Software that is public domain from USGS (Philips 1997) and OASIS montaj<sup>TM</sup> Data Processing and Analysis system (Geosoft 1997).

The magnetic data were transformed to the wavenumber domain. Reduction to the north magnetic pole was performed at the first stage of processing of aeromagnetic data. Reduced to the North Pole map of Philippi is shown in Figure 3. The azimuthally averaged logarithmic power spectrum was computed (Fig. 4). The log spectrum shows two parts. The spectral slope technique of Spector and Grant (1970) was applied to each. A depth estimate of about 1 km for the higher wavenumber part and 3.65 km for the lower wavenumber part was calculated.

Horizontal gradient maxima (Fig. 5) used to reveal the horizontal boundaries of the sources. According to Blakely and Simpson (1986) and Grauch and Cordell (1987) the maximum values of horizontal gradient will be located near vertical sides. Eastern flank is well depicted from the horizontal gradient maxima map. Cordell and McCafferty (1989) have presented an iterative method to transform the potential field data into uniform domains separated by abrupt domain boundaries. The method was called "terracing" for obvious reasons and comprises a mapping of the physical property, which caused the anomalous field. Although the method is directly applicable to the gravity field

data, the magnetic data have to be subjected to pseudogravity transform first. Terracing method used in conjunction with horizontal gradient maxima to delineate the body boundaries. Figure 6 shows the "terraced" magnetic field.

The magnetic field was differential continued upwards to 3.275 km above sea level (Fig. 7), using the method of Ivan (1994). In order to accomplish the later the topography was grided at the same grid locations. The upward continued field was used to verify model's validity.

A regional field was removed from the gravity data. Horizontal gradient maxima and "terracing" methods were applied to gravity field to assist modelling.

### INTERPRETATION OF THE ANOMALOUS POTENTIAL FIELDS

Three profiles, shown in Figure 8, were extracted from the residual Bouguer anomaly map, perpendicular to the basin's major axis. This axis is 40 km long. Profile (L3) passes over the granitic intrusion, so a magnetic profile was also extracted from the reduced to the pole total field anomaly map. A regional field was extracted from each profile, in order to remove the effect of the surrounding rocks. The data were inverted using SAKI (Webring, 1985), and 2 1/2-D models were created. The result from the enhancement techniques which were described in a previous paragraph, were used to put constraints in the model parameters.

The model for profile (L1) is shown in Figure 9. The maximum depth to the basement for this profile is 1.8 km. Profile (L2) passes over the deeper part of the basin. Model for profile (L2) is shown in Figure 10, where the maximum depth to the basement is 5.36 km. End corrections were applied to both profiles. Profile (L2) has fore end set to 30 km and back end set to 10 km, while profile (L2) has both fore and back ends set to 20 km.

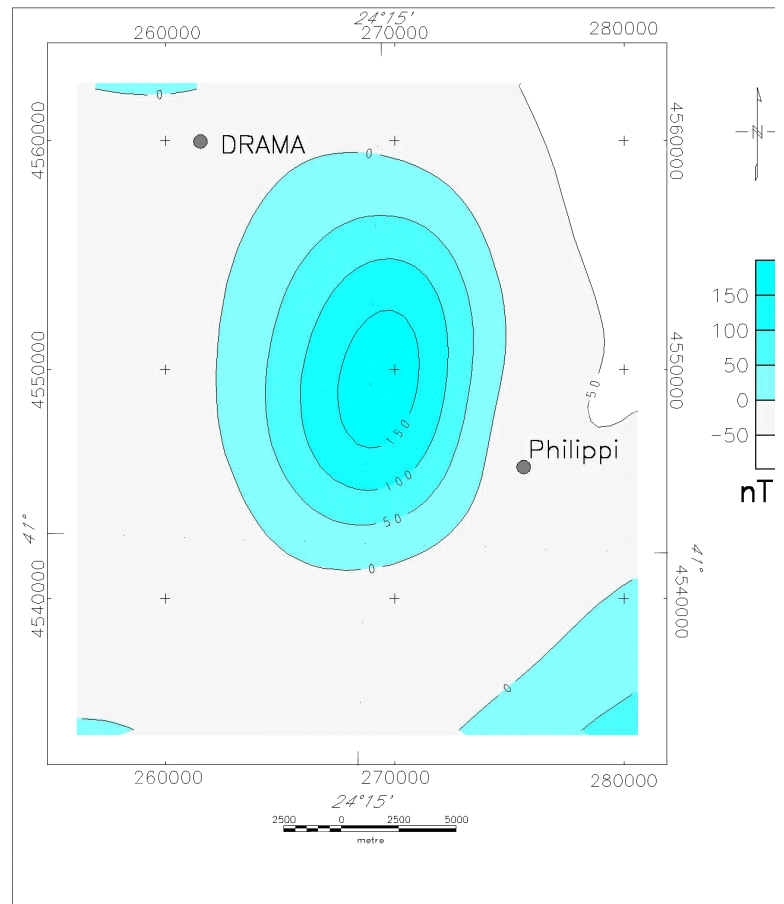


**FIG. 7.** Differential upward continued magnetic field at the absolute altitude of 3.275 m.

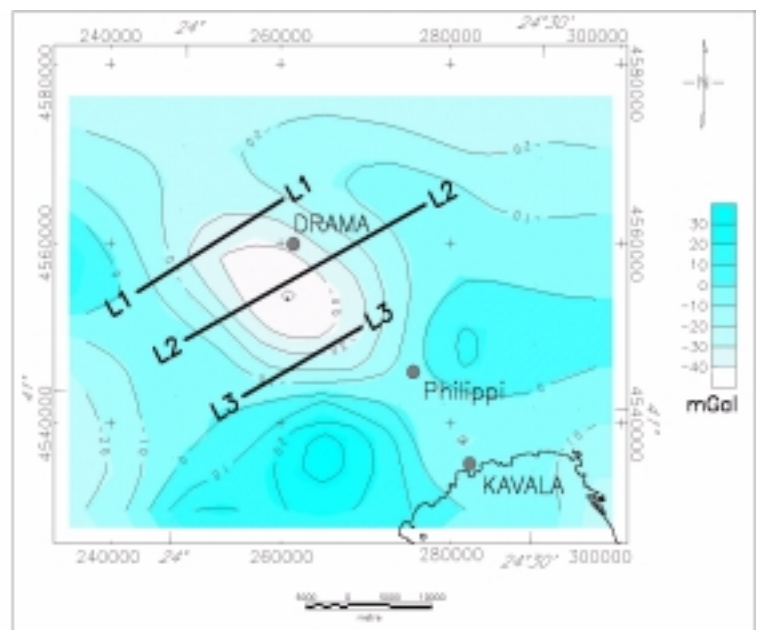


**FIG. 8.** Residual Bouguer anomaly map of Philippi basin. The lines selected for modeling are also shown.

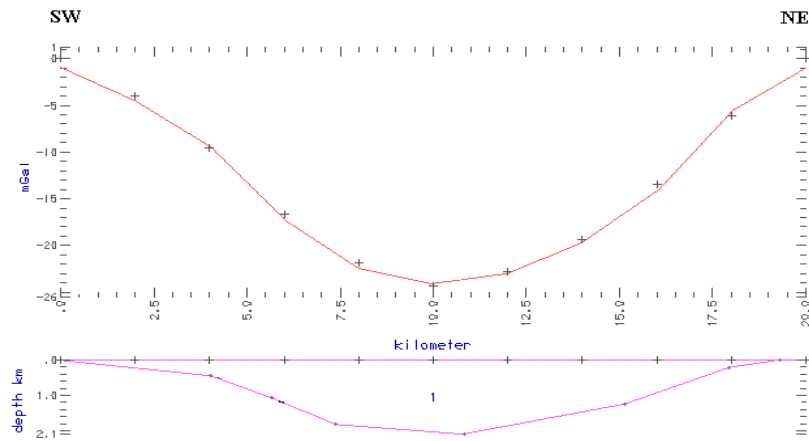


**FIG. 9.** Gravity model for line (L1) (bottom). The crosses show the observed field, while the solid line depicts the computed effect of the model.

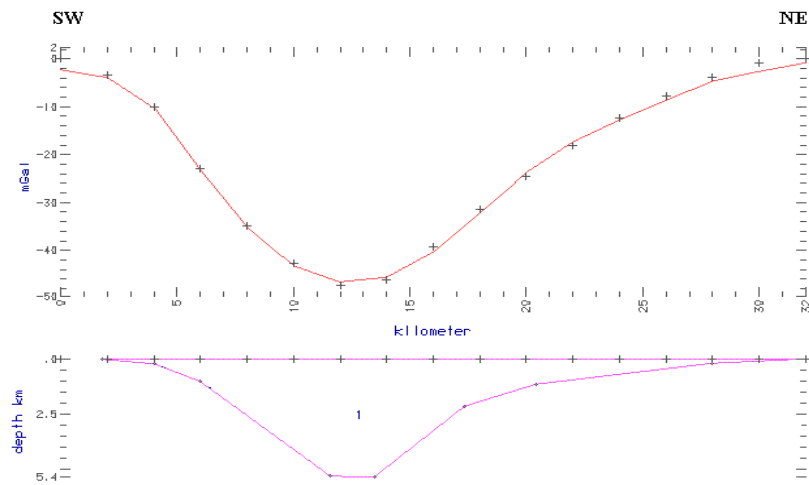


**FIG. 10.** Gravity model for line (L2) (bottom). The crosses show the observed field, while the solid line depicts the computed effect of the model.

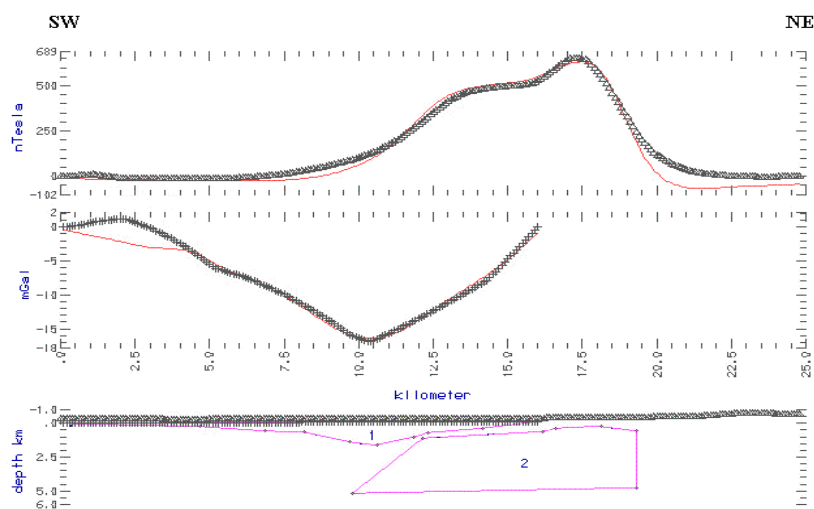


**FIG. 11.** Gravity and magnetic models for line (L3) (bottom). The crosses show the observed fields, while the solid lines depict the computed effect of the models. Body 1 is the sedimentary infill and body 2 is the granite.

The model for profile (L3) is shown in Figure 11. The close relation of the Oligocene intrusion and the Miocene basin can be observed. Maximum depth to the basement for the sediments is 1.6 km, while depth to the top for the intrusion is 0.2 km and depth to the bottom 5.1 km (absolute depth). The prism of the sedimentary infill has fore end set to 10 km and back end set to 30 km, while the granitic prism has both fore and back ends set to 5 km.

The method of Hansen and Wang (1988) was used to create a forward three-dimensional model of the reduced to the north magnetic pole anomaly associated with the Philippi granitoid (Fig. 3). The method uses the expressions of the gravity and magnetic fields in the Fourier domain (Pedersen, 1978) to model homogeneous polyhedral bodies. These expressions can be written as sums of contributions from the vertices of the body in such way as to yield an efficient, flexible modeling algorithm. The results from this algorithm are very fast and accurate.

The Philippi intrusion 3-D model consists of three parts. The major part is a polyhedron having a flat bottom at 5.5 km, near the vertical eastern flank, probably caused by faulting and gentle west flank. The top of this major polyhedron is at 1 km. From there two smaller parts continue towards the surface. Dome (A) reaches 0.5 km under the surface, while Dome (B) goes a bit further to 0.3 km. Small veins from these bodies are cropping out near Philippi village. The 3-D model has a good correlation with the 2 1/2-D for profile (L3). Zero level surface for this model was assumed to be the mean absolute altitude of the flight lines. The mean topographic altitude in Philippi basin and intrusion is 100 m. Figure 12 shows the 3-D model along with the field produced by this model.

The validity of the model was tested using the upward continued field. The new zero level surface was the upward continued one, that is 3275 m absolute altitude. Model's corners were adjusted

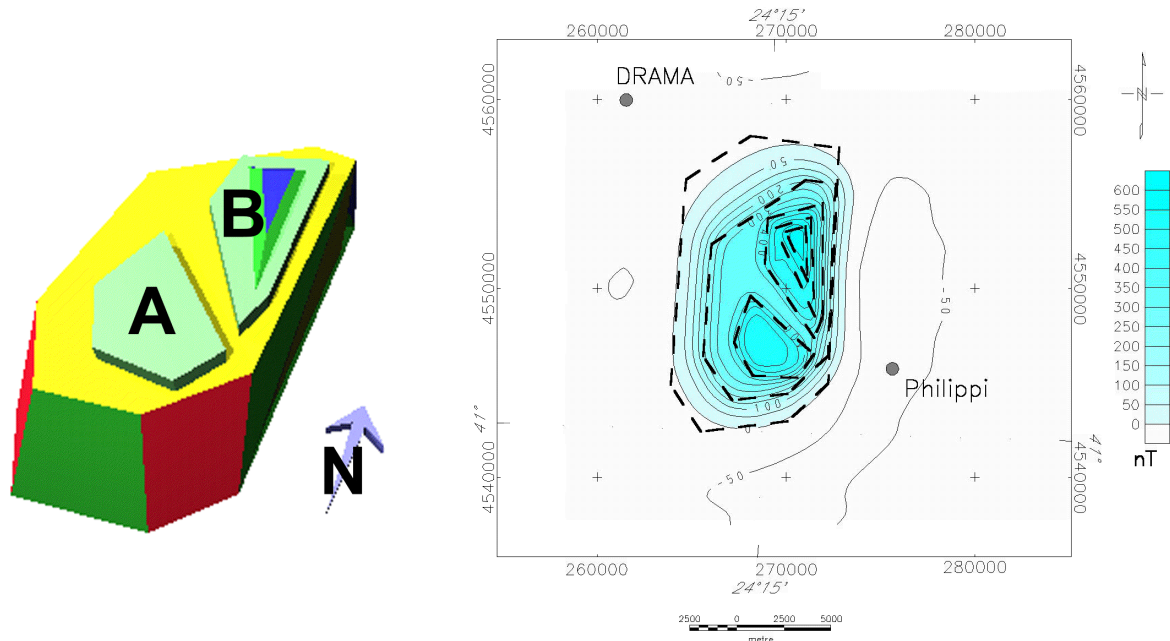


**FIG. 12.** The 3-D model of the Philippi granite in the left hand side. The computed effect of the model is shown in the right hand side. The dashed line depicts the horizontal plan view of the model prisms.

to the new surface and the model's field was calculated and compared with that of Figure 7. Figure 13 shows the effect of the model of Figure 12 at 3275 m absolute altitude.

## CONCLUSION

A large intrusion is interpreted to be the source of the magnetic anomaly at Philippi area. The bottom of the polyhedral body is at 5.5 km, while its top is close to the surface.

The sedimentary cover of Philippi basin causes the large negative anomaly in the Bouguer anomaly map. The bottom of the basin has a maximum depth of about 5.36 km.

## ACKNOWLEDGEMENT

The authors are greatly indebted to Dr. Abdulah Ates for his thorough criticism of the manuscript that improved the paper considerably.

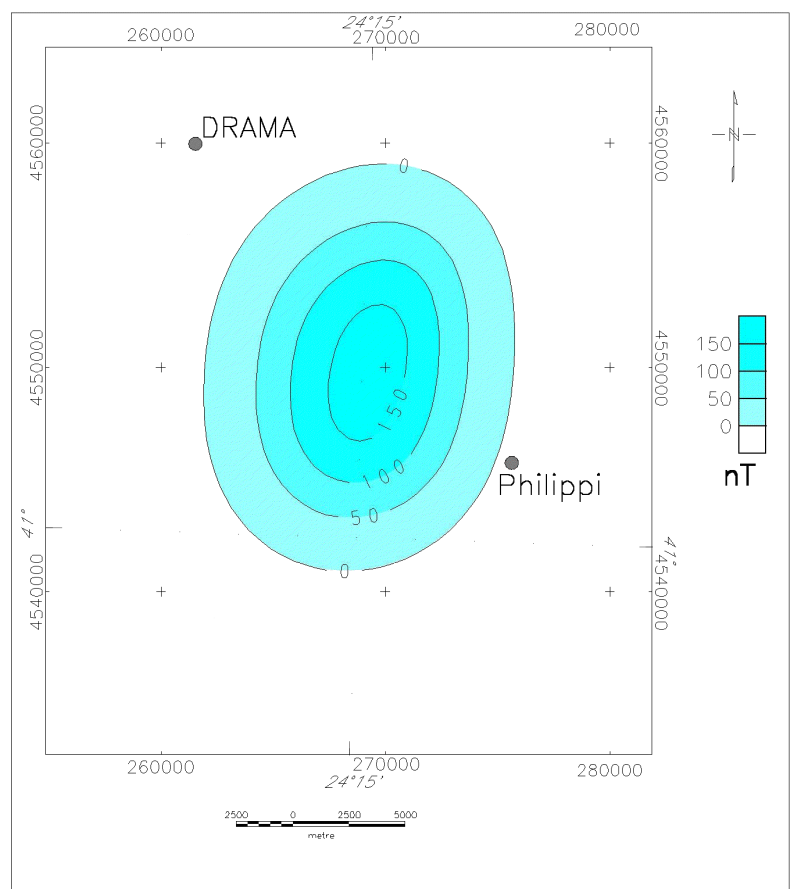


**FIG. 13.** The computed effect of the Philippi granite model at constant absolute altitude 3275 m. This field is in good comparison with that of Figure 7.



## REFERENCES

- ABEM, 1967. *Final Report*: On the airborne geophysical survey carried out for the Greek Institute for Geology and Subsurface Research during the year 1966 by ABEM: AB Elektrisk Malmletning, Stockholm, IGME, Athens.
- Atzemoglou, A., 1997. Paleomagnetic results from northern Greece and their contribution to the interpretation of the geodynamic evolution of the area during the Tertiary: Doctorate Thesis, Aristotle Univ. of Thessaloniki, 319 p.
- Bitzios, D., Constantinides, C., Dimadis, E., Dimitriades, A., Katirzoglou, C., and Zachos, S., 1981. Mixed sulphide mineralization of the Greek Rhodope. Report for the Greek-Soviet scientific cooperation in the field of Geology: IGME, Athens, 118 p.
- Blakely, R. J., and Simpson, R. W., 1986. Approximating edges of source bodies from magnetic or gravity anomalies: *Geophysics*, **51**, 1494-98.
- Cordell, L., and McCafferty, A. E., 1989. A Terracing operator for physical property mapping with potential field data: *Geophysics*, **54**, 621-634.
- Eleftheriadis, G., Pe-Piper, G., and Christofides, G., 1995. Petrology of the Philippi granitoid rocks and their microgranular enclaves (East Macedonia, N. Greece): *Geol. Soc. Greece, Sp. Publ.*, No. 4, 512-517.
- Geosoft, 1997. OASIS Montaj Data Processing and Analysis (DPA) System for Earth Science Applications, Version 4.1 user Guide: Geosoft Inc., pp. 290.
- Grauch, V. J. S., and Cordell, L., 1987. Limitations of determining density or magnetic boundaries from the horizontal gradient of gravity or pseudogravity data: *Geophysics*, **52**, 118-121.
- Hansen, R. O., and Wang, X., 1988. Simplified frequency-domain expressions for potential fields of arbitrary three-dimensional bodies: *Geophysics*, **53**, 365-74.
- Ivan, M., 1994. Upward continuation of potential fields from a polyhedral surface: *Geophysical Prospecting*, **42**, 391-404.
- Kronberg, P., Meyer, W., and Pilger, A., 1970. Geologie der Rilla-Rhodope Masse zwischen Strimon und Nestos (Nordgriechenland): *Geol. Jahrb. Beih.*, **88**, 133-180.
- Lagios, E., Chailas, S., Hipkin, R. G., and Drakopoulos, J., 1994. Gravity and Topographic Data Banks of Greece: University of Athens, Athens.
- Lyberis, N., 1984. Tectonic evolution of the North Aegean trough, In: "The Geological Evolution of the Eastern Mediterranean", edited by Dixon J. E. and Robertson A. H. F., The Geological Evolution of the Eastern Mediterranean: *Geol. Soc. Spec. Publ.*, 17, Oxford, Blackwell Scientific Publications, 709-725.
- Makris, J., and Stavrou, A., 1984. Compilation of gravity maps of Greece: Hamburg University, Institute of Geophysics, Hamburg, pp 12.
- Maltezou, F., and Brooks, M., 1989. A geophysical investigation of post-Alpine granites and Tertiary sedimentary basins in northern Greece: *Journal of the Geological Society, London*, 146, 53-59.
- Maltezou, F., 1987. Gravity and Magnetic Studies of the Rhodope Region, NE Greece: PhD Thesis, University of Southampton, U.K.
- Morelli, C., Gantar, G., and Pisani, M., 1975a. Bathymetry, gravity and magnetism in the strait of Sicily and the Ionian sea: *Boll. Geofis. Teor. Appl.*, **17**, 39-58.
- Morelli, C., Pisani, M. and Gantar, G., 1975b. Geophysical studies in the Aegean sea and in the eastern Mediterranean: *Boll. Geof. Teor. Ed Appl.*, **18**, 127-167.
- Papanikolaou, D., and Panagopoulos, A., 1981. On the structural style of Southern Rhodope: *Geol. Balc.*, **11**, 13-22.
- Pedersen, L. B., 1978. Wavenumber domain expressions for potential fields from arbitrary 2-, 2 1/2-, and 3-dimensional bodies: *Geophysics*, **43**, 626-30.
- Phillips, J. D., 1997. Potential-Field Geophysical Software for the PC, version 2.2: U.S. Geological Survey Open-File Report 97-725.
- Spector, A. and Grant, F. S., 1970. Statistical Models for Interpreting Aeromagnetic Data: *Geophysics*, **35**, 293-302.
- Stampolidis, A., 1999. The magnetic field of Macedonia and Thrace and its relation to the geological and geophysical structure of the area: Doctorate thesis, Aristotle University of Thessaloniki.
- Webring, M.W., 1985. SAKI--A Fortran Program for Generalized Linear Inversion of Gravity and Magnetic Profiles, Open-File Report 85-122, U.S.: Geological Survey.
- Zachos, S., and Dimadis, E., 1983. The geotectonic position of the Skaloti-Echinos granite and it's relationship to metamorphic formations of Greek Western and Central Rhodope: *Geologica Balcanica*, **13** (5), 17-24.